Active thermography based on tensor rank decomposition

Peter W. Spaeth*, Peter L. Takunju, and Joseph N. Zalameda

Nondestructive Evaluation Sciences Branch, NASA Langley Research Center

ABSTRACT

Principal Component Thermography applies Singular Value Decomposition (SVD) to post-process data that are derived from active thermographic inspections. SVD provides useful compression of the data and allows for better understanding of substructure and indications of potential damage. In the standard approach, SVD is applied to a certain reshaping of a three-dimensional data stack into a two-dimensional array. This work applies the CANDECOMP-PARAFAC (CP) tensor rank decomposition directly to the three-dimensional data to avoid the initial reshaping step in order to begin to develop an inspection method that can more accurately detect defects in non-homogeneous and anisotropic materials. Tests against simulated data that compare the CP decomposition method with traditional Principal Component Thermography based on SVD are described. Finally, the method of Proper Generalized Decomposition (PGD) is used to derive the CP decomposition, and its performance against other algorithms is also discussed.

Keywords: Active thermography, Singular Value Decomposition (SVD), CANDECOMP-PARAFAC (CP) Decomposition, Tensor Approximation, Proper Generalized Decomposition (PGD), Alternating Least Squares (ALS)

1. INTRODUCTION

Active thermographic inspections generate sequences of two-dimensional images that are indexed by time. The resulting data are passed to algorithms that identify substructures and indications of damage in the volume of interest, and the most common approaches taken in these algorithms use SVD in some form. For example, Rajic [1] introduced SVD for contrast enhancement in order to highlight defects in the volume of interest. Cramer and Winfree [2] introduced a fixed-eigenvector approach that combines a priori physics-based thermal models with SVD as a framework for data compression and defect recognition and quantification. In both cases input data are reshaped into two-dimensional arrays that can then be analyzed using traditional SVD. This is appealing for several reasons. First, SVD approximations are optimal in the sense that they provide the best low-rank approximation to the reshaped array. Second, the features computed using SVD are orthogonal, thus avoiding any potential difficulties arising from collinearity. On the other hand, the reshaping of the data into two-dimensional arrays, while practical, is somewhat artificial in that different factors can be combined in undesirable ways. In images, for instance, reshaping changes the local structure of neighboring pixels.

The purpose of exploring the methods in this paper is to avoid reshaping the data into an array so that different factors can be treated equally in the modeling steps with the goal of developing methods that can better quantify defects in non-homogeneous and anisotropic materials. In particular, the CP model is applied to construct features for defect quantification similar to the fixed eigenvector method. After introducing the necessary preliminaries, a comparison of the fixed eigenvector approach based on SVD versus one using CP tensor decompositions is examined for a one-dimensional thermal model.

2. SINGULAR VALUE DECOMPOSITION

Among its many applications, SVD is used for dimensionality reduction, optimal low-rank approximation of matrices, least squares optimization, and reduced order modeling of complex physical systems. And because numerical methods to compute the SVD are highly mature, SVD is an indispensable tool in the application of data science to problems in science and engineering.

*E-mail: peter.w.spaeth@nasa.gov; Telephone: +1 (757) 864-5415

The singular value decomposition of a real $m \times n$ matrix $M = (m_{ij}) \in \mathbb{R}^{m \times n}$ is

$$M = U \Sigma V^T, \tag{1}$$

where U and V are orthogonal matrices of dimensions $m \times m$ and $n \times n$, and Σ is an $m \times n$ rectangular diagonal matrix with non-negative diagonal entries $\sigma_k = \Sigma_{kk}$, such that $\sigma_1 \geq \sigma_2 \geq \cdots \geq \sigma_r \geq 0$. Equation (1) can also be written as

$$M = \sum_{k=1}^{r} \sigma_k U_k \cdot V_k, \tag{2}$$

where $U_k \cdot V_k$ denotes the outer product of columns of U and V, and $r \leq \min(m, n)$ is the rank of M. Figure 1 contains a schematic representation of Equation (2).

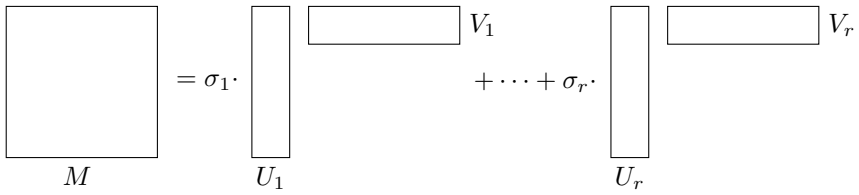

Figure 1. Singular Value Decomposition of a real matrix M.

Denote $B_k = U \Sigma_k V^T$, where Σ_k is the $m \times n$ rectangular matrix with diagonal elements equal to $\sigma_1, \ldots, \sigma_k$ and all other entries equal to zero. If

$$\|M\|_F = \left(\sum_{i,j} m_{ij}^2 \right)^{1/2}$$

denotes the Frobenius norm of M, then by the Eckart-Young theorem, for each $k = 1, 2, \ldots, r$, the matrix B_k satisfies

$$\|B_k\|_F = \inf_S \{ \|M - S\|_F \mid \text{rank } S = k \} = \left(\sum_{j=k+1}^{r} \sigma_j^2 \right)^{1/2}. \tag{3}$$

Hence the SVD gives the best rank-k approximation of M for each $k = 1, \ldots, r$. Conversely, the SVD of a matrix M can be computed as a recursive optimization problem. See Bisgard [3] for complete details.

3. CANDECOMP-PARAFAC APPROXIMATION

Now consider a third-order tensor $T \in \mathbb{R}^{m \times n \times p}$, which can be considered as a three-dimensional generalization of a matrix. There are many different approaches to generalize the SVD approximation of matrices to tensors; a comprehensive survey is given by Kolda and Bader [4]. The CP decomposition generalizes Equation (2) by looking for a collection of vectors x_l, y_l, and z_l of appropriate dimensions such that

$$T \cong \sum_{l=1}^{r} x_l \cdot y_l \cdot z_l. \tag{4}$$

The tensor T and its CP decomposition are shown conceptually in Figure 2.

By normalizing the vectors x_l, y_l, and z_l, Equation (4) can be rewritten as

$$T \cong \sum_{l=1}^{r} \lambda_l x_l \cdot y_l \cdot z_l. \tag{5}$$

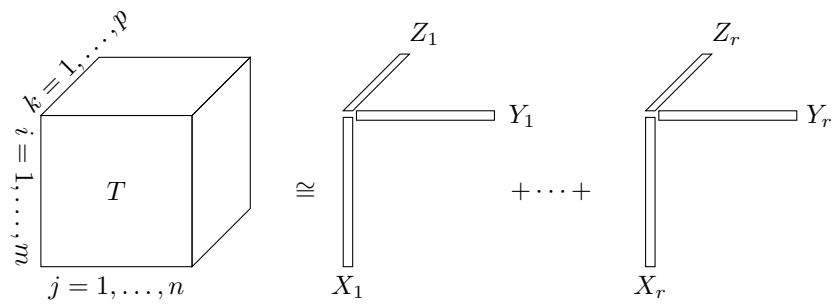

Figure 2. Order-three tensor $T \in \mathbb{R}^{m \times n \times p}$ and its CANDECOMP-PARAFAC (CP) decomposition.

Although Equations (2) and (5) have a similar form, the analogue to the Eckart-Young theorem for tensors does not hold in general. See [4] for additional details. Nonetheless useful tensor approximations can be computed using Equation (5) in the following sense. Fix r in Equation (5) and attempt to compute the tensor of the form $S_* = \sum_{l=1}^{r} \lambda_l x_l \cdot y_l \cdot z_l$ that minimizes the objective function

$$S \mapsto \|T - S\|_F. \tag{6}$$

In many instances, even when an optimal solution may not be found, approximate minimizers to Equation (6) can offer significant data compression. Indeed, whereas the data of the tensor T is of the size $m \cdot n \cdot p$, the CP-compressed representation given by S_* is of the size $r \cdot (n + m + p)$.

The standard approach to minimizing the objective in Equation (6) is based on the method of Alternating Least Squares (ALS) [5, 6]. In this paper, however, the PGD method is used to minimize Equation (6). The PGD is based on the method of weighted residuals. See Chinesta et al. [7] for additional details on PGD and its application to second-order tensor decompositions. Figure 3 shows the approximation error as a function of the number of terms r in Equation (5) computed using a Python implementation of PGD method for a random tensor of size $(25, 25, 25)$. For comparison, the approximation error based on the Kossaifi et al. [8] implementation of ALS is also included.

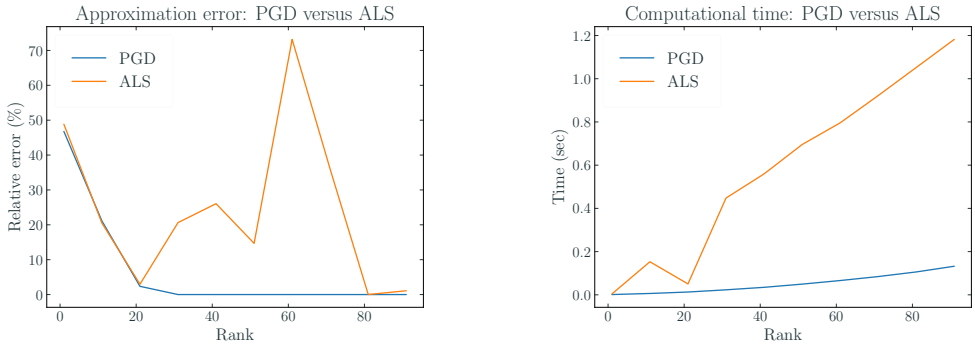

Figure 3. (*Left*) Residual error of the CP approximation as a function of the decomposition rank on a 3-tensor of size $(25, 25, 25)$ computed using PGD (shown in blue) versus ALS (shown in orange). (*Right*) Comparison of computational time of the CP decomposition of the same tensor based on the PGD method (in blue) versus the ALS method (in orange). ALS computed using the implementation of Kossaifi et al. [8].

In both cases, PGD and ALS provide excellent low-rank CP approximations to the tensor T. Note that the error for low-rank approximations is nearly equal for both methods up to rank 20, and the error is smaller for the PGD method across all ranks. This makes PGD a suitable choice for thermography applications where low-rank approximations and features are used. With respect to the Frobenius norm the rank 20 CP approximation of T is accurate to within 2% while requiring only approximately 10% of the size of T.

4. ONE-DIMENSIONAL MODEL

A one-dimensional thermal model without convection losses is used to evaluate an approach to thermography based on the CP tensor approximation versus the fixed eigenvector method developed by Cramer and Winfree [2]. In particular, the model describes the surface temperature response to a flash heat input of a multilayer material with an interior defect that is represesnted as a thermally resistive interface. To that end, consider a homogeneous plate of thickness d and thermal diffusivity α that contains an interface at a depth l with thermal resistance R. Assume the plate is insulating at $x = d$, with initial temperature 0 for all x and is subject to a Dirac heat pulse with energy Q at time $t = 0$. See Figure 4.

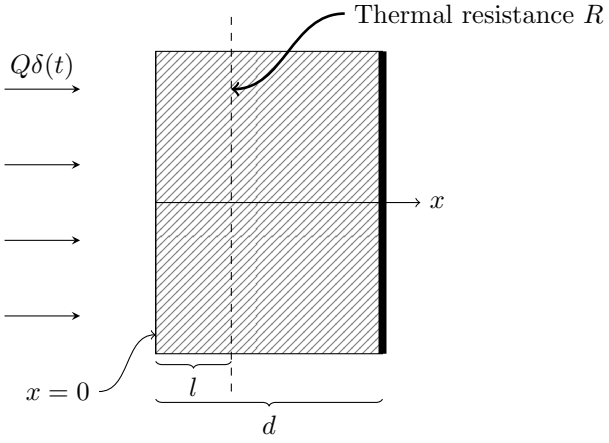

Figure 4. Finite thickness plate with Dirac heat pulse and resistive interface.

Let $u_1(x,t),\ 0 \le x \le l$ and $u_2(x,t),\ l \le x \le d$ represent the temperature of the plate respectively, in front of and behind the interface at $x = l$. The functions u_1 and u_2 satisfy the following set of equations:

$$\frac{\partial^2 u_i}{\partial x^2} = \frac{1}{\alpha}\frac{\partial u_i}{\partial t} \qquad u_i(x,0) = 0 \quad i = 1,2 \tag{7}$$

$$\frac{\partial u_1}{\partial x}(0,t) = -Q\delta(t) \qquad \frac{\partial u_2}{\partial x}(d,0) = 0 \qquad \frac{\partial u_1}{\partial x}(l,t) = \frac{u_1(l,t) - u_2(l,t)}{R} = \frac{\partial u_2}{\partial x}(l,t). \tag{8}$$

If the function θ_i defined by

$$\theta_i(x,\rho) = \int_0^\infty u_i(x,t)\, e^{-\rho t}\, dt$$

denotes the Laplace transform of u_i, then a straightforward calculation (cf. Carslaw, et al. [9]) shows that $\theta_1(0,\rho)$ satisfies

$$\theta_1(0,\rho) = \frac{Q}{q\Delta}\left(Rq\left(e^{2ql} + e^{4ql} - e^{2qd} - e^{2q(d+l)}\right) + 4e^{ql}\right), \tag{9}$$

where $q = \sqrt{\rho/\alpha}$ and

$$\Delta = Rq(-e^{2qd} - e^{4ql} + e^{2ql} + e^{2q(d+l)} + 2(e^{2ql} - e^{2q(l+d)})).$$

Figure 5 shows the surface temperature response in two settings. At left the interface depth is varied from $l = .375d$ to $l = .95d$ for fixed contact resistance $R = 1/(2\alpha)$, while in the plot on the right, the interface depth is fixed at $l = 0.5d$ and the contact resistance is reduced from $R = 10/(2\alpha)$ to $R = 1/(2\alpha)$. To estimate the surface temperature response $u_1(0,t)$, the inverse Laplace transform of θ_1 is computed numerically in Python using de Hoog's method [10].

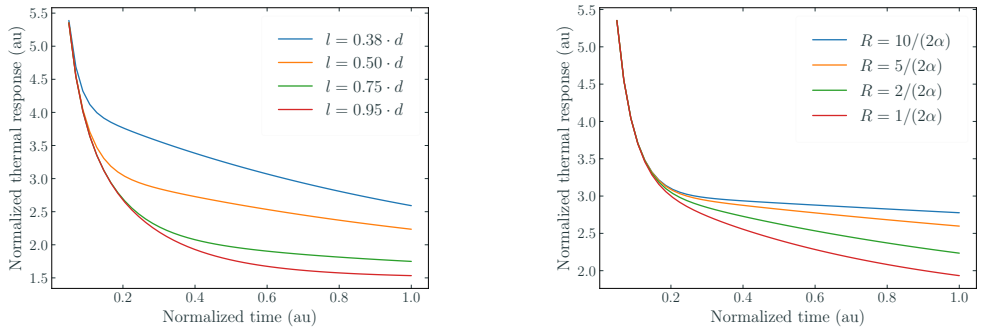

Figure 5. Normalized surface temperature for varying interface depth (at left) and varying thermal resistance (at right).

5. SIMULATION AND RESULTS

A discrete thermal model represented by a three-tensor T can be defined using the surface temperature response model in Section 4 as follows. Choose depths $l_1, \ldots, l_m$, resistances $R_1, \ldots, R_n$ and times $t_1, \ldots, t_p$, and set $T_{ijk} = u_1(0, t_k; l_i, R_j)$, where $u_1(0, t; l, R)$ denotes the surface temperature response at position $x = 0$ and time t for the given parameters l and R. Again the surface temperature response is computed numerically using de Hoog's method [10]. Similar to the fixed eigenvector approach, the tensor T is mean-normalized over the time dimension, i.e.

$$\bar{T} = T - \mu(T) \tag{10}$$

where $\mu(T)$ is the three-tensor with entries $\mu(T)_{ijk} = \frac{1}{p} \sum_{k=0}^{p} T_{ijk}$.

The PGD method provides a CP approximation to $\bar{T}$ of the form

$$\bar{T} \cong \sum_{l=1}^{r} \lambda_l X_l \cdot Y_l \cdot Z_l. \tag{11}$$

Figure 6 shows the first four PGD vectors $Z_1, \ldots, Z_4$ and the first ten PGD singular values $\lambda_1, \ldots, \lambda_{10}$ computed from the PGD approximation of the tensor $\bar{T}$ in Equation (11). To define T, 28 simulations corresponding to $m = 4$ different depths and $n = 7$ different values of the thermal resistance were computed across $p = 20$ time steps. The Z-components describe the temporal variation in the discrete thermal model T. Note 4 orders of magnitude decrease in PGD singular values one to four.

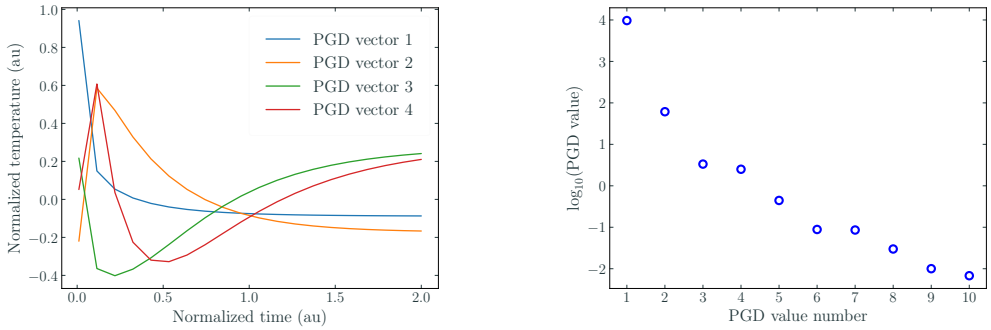

Figure 6. At left the time components of the four PGD vectors corresponding to the largest PGD singular values, the first 10 of which are shown at right.

Motivated by [1] and [2] the CP decomposition can be used to create summary features from a surface temperature profile by projection to the linear space spanned by the vectors $Z_1, \ldots, Z_r$. For example, if $u = u(t_k), k = 1, \ldots, p$ denotes a generic surface temperature at discrete times $t_1, \ldots, t_p$, then its associated features are given by the matrix product

$$\phi = Z^T \cdot u \in \mathbb{R}^r, \tag{12}$$

where Z is the matrix with columns $Z_1, \ldots Z_r$.

Using the same PGD vectors shown in Figure 6 that are derived from the 28 simulations described above, feature vectors $\phi_{ij} \in \mathbb{R}^4$ were computed for all temperature profiles $T_{ij:}$, where $T_{ij:}$ denotes the temperature profile corresponding to depth l_i and resistance R_j. The resulting collection of features can be used to estimate depth and thermal resistance as follows. Given the temperature profile u with feature vector ϕ associated to an unknown depth and resistance, its estimated depth $\widehat{l}$ is the depth associated to the nearest computed feature $\phi_{ij} \in \mathbb{R}^4$, i.e. $\widehat{l}_{CP} = l_{i_*}$ such that

$$i_* = \arg\min_i \{\|\phi - \phi_{ij}\| \mid i = 1, \ldots, m, j = 1, \ldots, n\}.$$

The same procedure for estimating depths can be carried out using the SVD of the reshaped matrix M of dimension 28×20, whose rows correspond to $T_{ij:}$. The only change is to use the matrix V whose columns consist of the right eigenvectors $V_1, \ldots, V_4$ corresponding to the four largest singular values of M rather than the PGD derived matrix Z. Figure 7 shows the performance of the CP depth estimation using the PGD derived feature vectors against the standard SVD approach from [2] applied to the reshaped matrix M. The plotted values correspond to the difference in absolute error $|l_{exact} - \widehat{l}|$ between the two methods, i.e.

$$\epsilon = |l_{exact} - \widehat{l}_{SVD}| - |l_{exact} - \widehat{l}_{CP}|. \tag{13}$$

Large positive values (shown in yellow) indicate pairs (l, R) where the CP method produces a better estimate of the interface depth compared with SVD. Although the SVD outperforms CP for most (R, l) pairs in this example, the CP method better estimates the depth of interfaces close to the back face and when the contact resistance is small.

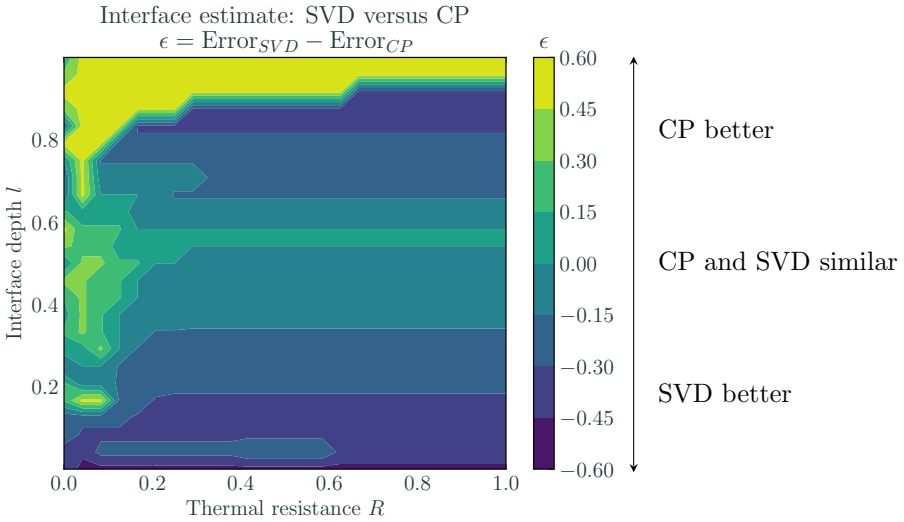

Figure 7. Comparing the two methods across varying interface depth and thermal resistance. Shown is the difference in error between the two methods. Regions with positive values correspond to locations for which the CP method performed best. In this example the SVD method performed best overall, but the CP method better predicts the depth of defects close to the maximum depth of the plate and when the thermal resistance is close to zero.

6. CONCLUSION

The results of this paper show that CP decomposition can be used to analyze the type of data arising in thermography and that the PGD method for computing the CP decomposition compares well against the standard ALS method for low-rank approximations of third order tensors. For such tensors of size (25, 25, 25) the CP approximation based on PGD produces an approximation of greater than 95% accuracy with a 90% reduction in size. In addition, the PGD method computes more accurate low-rank approximations more quickly than ALS, which makes PGD a suitable method for applications in thermography. The comparison of CP thermography to the fixed eigenvector SVD method shows that the CP method can in some circumstances perform as well as or better than the standard approach, but additional analysis will be needed to fully compare the two methods. In particular, evaluating the CP method against the standard fixed eigenvector approach on experimental data with known defects and on the two dimensional thermal model in [11] will be important next steps.

ACKNOWLEDGMENTS

The first named author thanks James Bisgard for helpful discussions about orthogonal tensor decompositions and the convergence of the ALS algorithm.

REFERENCES

[1] Rajic, N., "Principal component thermography for flaw contrast enhancement and flaw depth characterisation in composite structures," *Composite Structures* **58**(4), 521–528 (2002).

[2] Cramer, K. E. and Winfree, W. P., "Fixed eigenvector analysis of thermographic NDE data," in [*Thermosense: Thermal Infrared Applications XXXIII*], Safai, M. and Brown, J. R., eds., **8013**, 225 – 235, International Society for Optics and Photonics, SPIE (2011).

[3] Bisgard, J., [*Analysis and Linear Algebra: The Singular Value Decomposition and Applications*], Student Mathematical Library, American Mathematical Society (2020).

[4] Kolda, T. G. and Bader, B. W., "Tensor decompositions and applications," *SIAM Rev.* **51**, 455–500 (aug 2009).

[5] Carroll, J. D. and Chang, J.-J., "Analysis of individual differences in multidimensional scaling via an n-way generalization of "Eckart-Young" decomposition," *Psychometrika* **35**(3), 283–319 (1970).

[6] Harshman, R. A., "Foundations of the parafac procedure: Models and conditions for an "explanatory" multi-model factor analysis," (1970).

[7] Chinesta, F., Keunings, R., and Leygue, A., [*The Proper Generalized Decomposition for Advanced Numerical Simulations: A Primer*], SpringerBriefs in Applied Sciences and Technology, Springer International Publishing (2013).

[8] Kossaifi, J., Panagakis, Y., Anandkumar, A., and Pantic, M., "TensorLy: Tensor Learning in Python," *Journal of Machine Learning Research* **20**(26), 1–6 (2019).

[9] Carslaw, H., Jaeger, J., and Jaeger, J., [*Conduction of Heat in Solids*], Oxford science publications, Clarendon Press (1959).

[10] Johansson, F. et al., *mpmath: a Python library for arbitrary-precision floating-point arithmetic (version 0.18)* (December 2013). `http://mpmath.org/`.

[11] Winfree, W. P., Zalameda, J. N., and Gregory, E. D., "Application of the quadrupole method for simulation of passive thermography," in [*Thermosense: Thermal Infrared Applications XXXIX*], Bison, P. and Burleigh, D., eds., **10214**, 245 – 254, International Society for Optics and Photonics, SPIE (2017).